ORIGINAL ARTICLE

Influence of Electrolyte Concentration Variation on Thin Oxide Coating Production in Aluminum Alloy by PEO

Rafael Resende Lucas[1] · Luís Rogério de Oliveira Hein[1] · Edson Cocchieri Botelho[1] · Rogério Pinto Mota[1]

Abstract

Aluminum alloy 2024-T3 underwent Plasma Electrolytic Oxidation (PEO) treatment with sodium tetraborate solution at various concentrations. Coatings were characterized using SEM, EDS, XRD, and FT-IR. Increasing medium conductivity reduced power consumption. Alumina coatings exhibited dielectric properties, with reduced current and surface brightness during the process. Surface morphology displayed PEO characteristics, including micro-pores, remnants of discharge channels, spherical protrusions, and cracks. The coating thickness averaged 1.7 μm. XRD analysis showed a decrease in intermetallic phases and an increase in γ-Al_2O_3. Chemical analysis revealed a hybrid composition from substrate, electrolyte, and environment, including CO_2 due to Na^+ ions' affinity for adsorbing bidentate carbonate ions.

Keywords Plasma electrolytic oxidation · Aluminum alloy · Alumina · Surface treatment · Characterizations

Introduction

Aluminum alloys are extensively utilized owing to their reduced density, elevated electrical and thermal conductivities, and their inherent passivation capability, particularly about the alloy 1XXX. However, in scenarios necessitating their utilization in more resilient frameworks like ships, automobiles, and aircraft, additional elements are incorporated to enhance their mechanical robustness, thereby giving rise to alloys 2XXX, 3XXX, and so forth (Reis et al. 2021; Ghanaraja et al. 2018).

The AA2024 alloy was chosen for this study due to its various characteristics that make it extremely suitable for multiple applications. With its low density, the AA2024 alloy is ideal for use in vehicles. Additionally, its high thermal and electrical conductivity makes it versatile in various industrial sectors. The affordable cost of the AA2024 alloy also contributes to its viability in both experimental and commercial contexts (Ghanaraja et al. 2018; Ansari et al. 2018; Lucas et al. 2022).

Nevertheless, it is essential to note that aluminum, despite its benefits, exhibits the property of being relatively malleable and prone to abrasions. Consequently, it frequently necessitates surface modifications to enhance its surface toughness. Anodizing stands out as one of the most prevalent techniques, entailing electrochemical procedures. Nevertheless, it is crucial to highlight that anodization may present a challenge in terms of environmental and health implications, attributed to the utilization of potentially hazardous and carcinogenic acidic solutions (Lucas et al. 2022; Yerokhin et al. 2004).

Plasma Electrolytic Oxidation (PEO), also known as Micro Arc Oxidation (MAO), is an electrochemical conversion treatment, which the main aim is to create on passive alloys (Al, Mg, Ti, Nb etc.) oxide coatings, with better chemical and physical properties than those developed by conventional electrochemical processes, in addition to being more efficient from an environmental point of view, by employing alkaline solutions, based on silicates, phosphates, borates, etc. that help reduce environmental impacts (Zinigrad and Kossenko 2015; Khiabani et al. 2021; Lucas et al. 2020; Yerokhin et al. 1999).

In the same manner as the traditional anodizing method, the PEO process is significantly influenced by various operational parameters. These parameters include the composition of the alloy being treated, the duration of treatment, the electrical conditions during treatment, the electrolyte's chemical composition, as well as any additives used. When focusing on the electrolyte aspect, it is not

✉ Rafael Resende Lucas
   rr.lucas@unesp.br

[1] São Paulo State University (UNESP), School of Engineering
     and Sciences, Guaratinguetá, São Paulo, Brazil

uncommon to encounter in scholarly works, procedures that incorporate the usage of sodium silicate (Na_2SiO_3). This particular compound is known to generate a highly efficient oxidative film on both aluminum and magnesium substrates. The resulting film exhibits a distinct dual-layer morphology. The first layer is thin and closely adherent to the underlying substrate, while the second layer is more porous and constitutes a significant portion, ranging from 60 to 80%, of the overall thickness of the PEO coating (Yerokhin et al. 2004; Khiabani et al. 2021; Sopchenski et al. 2020; Shore et al. 2021).

In this study, the AA2024 alloy (Alclad) was submitted to PEO treatment, using a sodium tetraborate electrolyte ($Na_2B_4O_7$), in four different concentrations: 1, 5, 10 and 15 g/L. The objective was to investigate the influence of these concentrations on the plasma, measuring the average power consumed, and also on the characteristics of the coatings generated, including thickness, crystalline phase, morphology of the coatings, microhardness, and chemical composition. This study was conducted to provide additional information on the electrolyte concentration parameter in the PEO treatment and contribute to the literature in this area.

Experimental Procedure

Preparation of Samples and Treatment Solutions

Samples with dimensions of $25 \times 25 \times 3.5$ mm of aluminum alloy 2024 (Alclad) were cleaned with neutral detergent for 15 min, followed by ultrasonic cleaning in isopropyl alcohol for 15 min.

The elemental makeup (by weight) of the employed alloy in the role of a provider includes less than 0.5% silicon, less than 0.5% iron, 3.8–4.9% copper, 0.3–0.9% manganese, less than 0.1% chromium, less than 0.25% zinc, less than 0.15% titanium, with the remaining portion consisting of aluminum.

Alkaline solutions (pH 9.1) of sodium tetraborate ($Na_2B_4O_7$) were prepared to assess the effect of electrolyte concentration variation on the oxide coating, with concentrations of 1; 5; 10 and 15 g/L. Although sodium tetraborate (Na_2BO_4) is used as an additive (in small quantities) with other salts, as commonly employed with sodium silicate (Na_2SiO_3), which ensures thicker coatings and microstructures more characteristic of PEO processes, depending on the adopted parameters, it makes the coating fragile when subjected to shear forces (Shore et al. 2021). All solutions underwent ultrasonic homogenization for 15 min. The electrolyte used was obtained from Dinâmica Ltda Company, with a purity of 99%.

Surface Treatment by Plasma Electrolytic Oxidation (PEO)

The experimental system assembled to perform this treatment consists of: a voltage variator (0–200 V); a voltage rectifier bridge (KBPC 5010); two electrolytic capacitors of 2400 µF/450 V each one, to double the rectified voltage; two multimeters to monitor the voltage and electric current in the system were used; a glass Becker (2000 mL) was used as electrolytic tub; an AA1200 aluminum counter electrode; and a thermometer to monitor the evolution of the treatment temperature. In the system, the sample was arranged with 30 mm from the counter electrode, the working voltage was constant (350 V) for 300 s as shown in Table 1.

Characterizations

The conductivity of the electrolyte used was evaluated by a portable Knup conductivity meter, model KP AA008, with a range of 0–9999 µs/cm. The thickness of the coating was evaluated by the eddy current method, using an Instrutherm meter, model ME 250, with a range from 0 to 1250 µm and resolution of 0.1 µm, performing 10 measurements along the surface, based on the ISO 2360 standard. Substrate mass variation was measured using a SHIMADZU analytical balance, model AUY220, with an accuracy of 0.1 mg. The crystalline phase of the coatings was evaluated by X-ray diffractometry, with a Bruker diffractometer, model D8 advance, at $2(\theta)$ with a range of 15°–90°, step of 0.05°, voltage of 40 kV and current of 40 mA.

The surface morphology of the oxide coatings was evaluated by scanning electron microscopy (SEM), being model EVO LS15 from the manufacturer Zeiss, together with EDS analysis was used to quantify the constituent elements in the coating. The molecular structure of the oxides generated was evaluated by an ATR FTIR spectrometer, Perkin Elmer Spectrum 100, covering functional groups of 1000–650 cm^{-1}, with 128 scans and resolution of 4 cm^{-1}.

Table 1 Parameters for plasma electrolytic oxidation treatment

Sample	Time (s)	Voltage (V)	$Na_2B_4O_7$ (g/L)
A	300	350	1.0
B			5.0
C			10.0
D			15.0

Results and Discussions

Current Treatment Variation

Because the PEO treatment occurred in potentiostatic mode, it is observed that the current varies over the treatment time (left side), and the variation in current density is also noticeable in the plasma appearance (right side), as shown in Fig. 1.

The escalation in the electrical resistance within the system stems from the generation of an alumina dielectric film on the substrates' surface, thereby elevating the electrolyte's temperature. Within this investigation, all interventions exhibited a temperature surge of approximately 3 °C, albeit below 25 °C. Upon scrutinizing the plot, one can observe a zenith near the 30-s mark (1*), denoting the juncture of maximal current density during the procedure. At this phase, the specimen displays a conspicuous luminosity; nevertheless, as the procedure advances, this luminosity gradually diminishes (up to 3*), presumably due to the augmentation in the oxide coating's thickness. Beyond 90 s, the current density either stabilizes or exhibits minimal fluctuations up to 300 s. Previous researchers have documented the manifestation of the current decline phenomenon during plasma electrolytic oxidation treatment, employing the constant voltage process (potentiostatic) (Lucas et al. 2022; Lucas et al. 2020; Xue et al. 2014).

Average Power Consumed

As in the system specified in this work, it has a constant voltage and the current decreases rapidly over time, due to the formation of the dielectric layer, the calculated power will be the average power, deduced by Eq. 1.

$$P_m = \frac{1}{t}\int_{t0}^{t} p(t)dt = \frac{1}{t}\int_{t0}^{t} V(t)j(t)dt \tag{1}$$
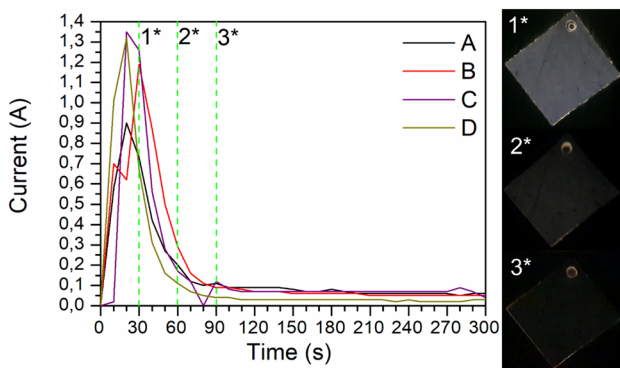
Sendo: *Pm*: power consumed [watts]; t: Time [seconds]; V: voltage [volts]; j: current density [A/m^2].

Table 2 and Fig. 2 present the average power used in each process. It is observed that power consumption increases with the increase in electrolyte concentration from 1 to 10 g/L; however, when evaluating the 15 g/L electrolyte, a decrease in consumption is observed due to the increased conductivity of the medium, which improves the movement of ions in the solution.

A close relationship is observed between conductivity and the electrical consumption of the system, being inversely proportional between processes C and D. This effect is observed during the PEO process when the so-called "sparking" occurs, theoretically indicating that the oxide coating has reached a limit thickness, and there is only oxide development in a few regions on the surface (Xue et al. 2014; Mohedano et al. 2021).

The "sparking" phenomenon occurs when the system current (Fig. 1) reaches 0.1 A and remains stable until the end of the process (300 s). Electrolyte D (15 g/L) reached this value earlier, which could justify its lower electricity consumption (Mohedano et al. 2021).

Table 2 Electric power consumption during the PEO treatment process

Sample	Na$_2$B$_4$O$_7$ (g/L)	Conductivity (mS/cm)	Power Consumed (kWh)
A	1.0	1.57	5.15
B	5.0	2.74	5.58
C	10.0	4.25	6.07
D	15.0	7.82	4.11

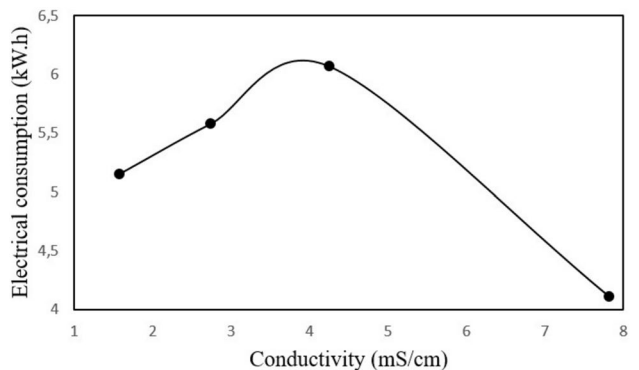**Fig. 1** Variation of the treatment current with plasma aspect

Fig. 2 Ratio of electrical conductivity vs. average power consumed

Surface Morphology and Chemical Composition of PEO Coatings

Figure 3 shows the surface morphology of the AA2024 alloy, treated with different concentrations of sodium tetraborate solution ($Na_2B_4O_7$).

The morphology of the coatings produced is typical of the electrolytic plasma process, with a multilayer surface, micro cracks, pores and nodular microstructures. Pores located randomly in the coatings are remnants of channels and discharge, in which the oxide material (alumina) was melted and ejected from the metal/coating interface, being quickly cooled when in contact with the electrolyte, also resulting in the formation of micro-cracks. It is observed that if also micro particles of melted oxide, randomly distributed on the studied surface, other authors also reported such morphologies in their studies (Dehnavi et al. 2013; Kikuchi et al. 2020; Mengesha et al. 2020; Duan et al. 2007).

The cultured oxide layer presents a seemingly more compact surface because the electrolyte has in its composition only sodium tetraborate ($Na_2B_4O_7$), which according to the literature, results in more compact layers and with fewer concentrations of pores and microcracks in the coating (Mengesha et al. 2020).

Table 3 presents the basic composition of the oxide's coatings produced. It is observed that the oxide layer is formed by the majority element of the alloy, aluminum (Al), the oxygen developed by the treatment and the ease of bonding of aluminum with it, and the element Boron (B), from the electrolyte of sodium tetraborate ($Na_2B_4O_7$),

Table 3 Percentage of elements of PEO coatings

%	AA2024	A	B	C	D
Al	88.4	46.3	36.8	58.8	59
Cr	–	0.2	–	–	–
Na	–	–	0.6	–	1.1
O	6.9	43.5	39	40	38.3
Si	0.5	0.8	0.6	0.5	0.7

which has a strong tendency to add oxygen in the coating (Yerokhin et al. 1999; Duan et al. 2007).

The treatments that were administered demonstrated effectiveness in enhancing the concentration of surface oxygen in the alloy, facilitating the formation of alumina (Al_2O_3). The average increase in oxygen concentration was significant, rising from 6.9% (in the case of AA2024) to 40.2% in the treated alloy. Furthermore, various other constituent elements of the alloy, such as chromium (0.2%), iron (with fluctuations ranging from 0.3 to 8.8%), and silicon (with fluctuations between 0.5 and 0.8%), were identified during the procedure. These elements are detectable in the oxide layer because of the inherent characteristics of the treatment, which result in the expulsion of these elements from the matrix to the coating/electrolyte interface throughout the process (Yerokhin et al. 2004; Yerokhin et al. 1999; Zinigrad and Kossenko 2015).

Figure 4 presents the mass variation values of each substrate [A], and the average thickness of the oxide coatings [B]. It is observed that the deposited oxide mass varies on all substrates, and the treatment with 10 g/L (C)

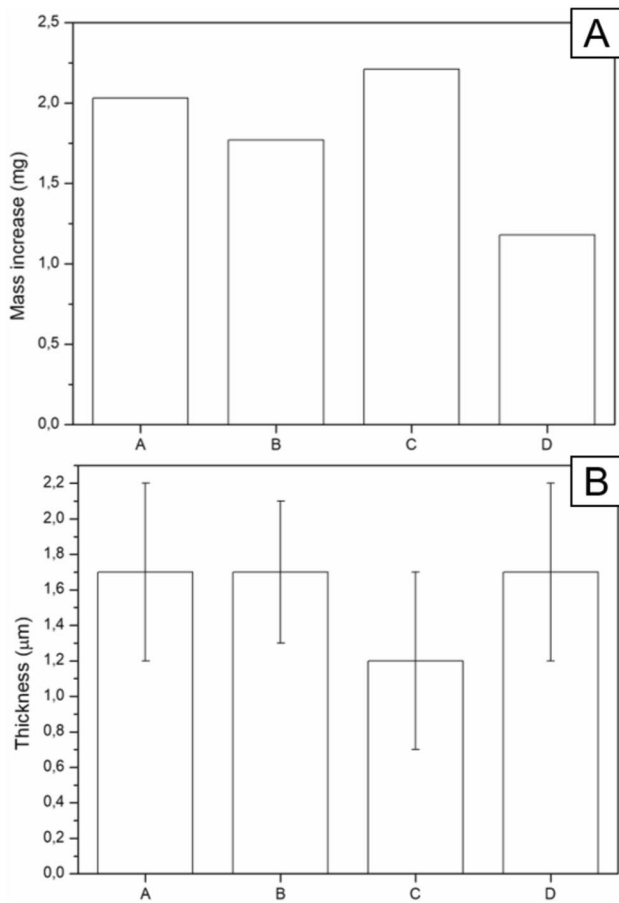**Fig. 3** Surface morphology of the treated samples: **A** (1 g/L); **B** (5 g/L); **C** (10 g/L) and **D** (15 g/L)
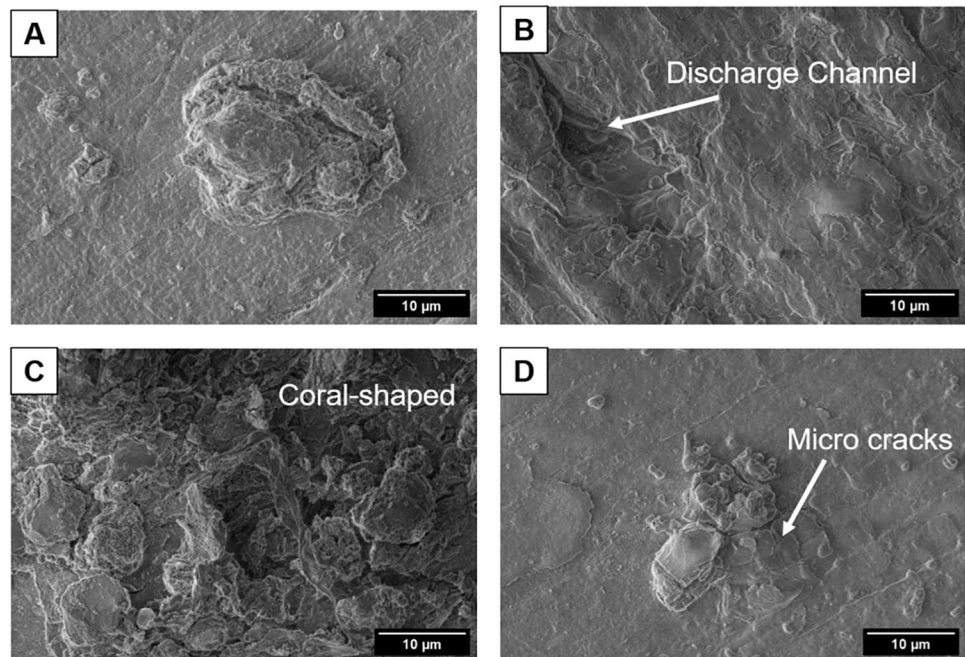
Fig. 4 Increase in mass in samples (**A**) and thickness of the oxide coating (**B**)

Fig. 5 X-ray diffractometry spectrum of the treated and untreated AA2024 alloy

showed the best deposition (2.21 mg). The variation in electrolyte concentration did not significantly alter the thickness of the coatings. Among all samples, only the sample treated with 10 g/L presented a thinner coating compared to the others (1.2 μm).

Nevertheless, from a statistical perspective (taking into account the standard deviations), it can be noted that the thickness of all samples hovers around 1.7 μm. Upon analysis of the data, it becomes apparent that coating C (10 g/L) exhibits a denser coating, with a reduced thickness compared to the rest and a higher degree of mass fluctuation (in g/cm^3). The presence of borate in their composition typically leads to the formation of a more condensed coating (Duan et al. 2007; Fermine, et al. 2023; Wierzbicka et al. 2022).

Taking into account the effective deposition time, that is, the point in time at which the system current reached 0.1 A, was 95, 85, 95, and 60 s for A, B, C, and D treatments, respectively. It is observed that the C process (10 g/L) had a higher deposition rate, about 23.3×10^{-3},
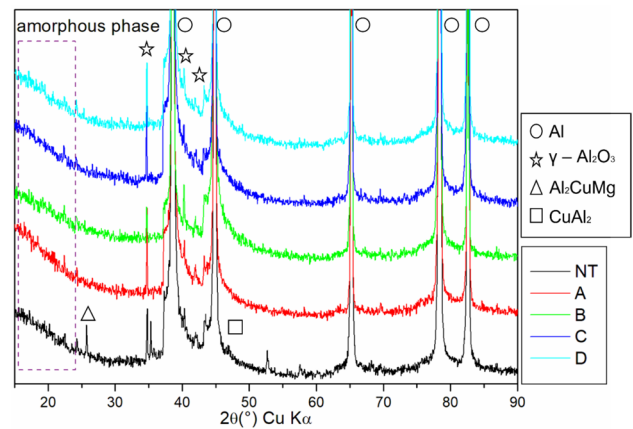
against 21.4×10^{-3}; 20.8×10^{-3}, and 19.7×10^{-3} mg/s of A, B, and D processes, respectively.

X-Ray Diffraction of PEO Coatings

Figure 5 (supplementary material) shown X-ray diffraction spectra of the untreated aluminum substrate (control sample—NT) as well as the treated samples. It is observed that, at the beginning of the spectra (15°–25°), there is a dip, originating from the amorphous phase of alumina, which is to the literature (Serdechnova, et al. 2017; Yang et al. 2019).

In the spectrum related to the untreated substrate (NT), peaks related to the intermetallic phases Al_2CuMg and Al_2Cu are noticed. These phases are detected due to remnants of elements from the alloy composition. When these phases are present in high concentrations, they lead to localized corrosion in alloys such as 2024, exhibiting a more anodic character compared to the metallic matrix (Ansari et al. 2018; Lucas et al. 2022; Yerokhin et al. 2004). With treated substrates, it is observed that these phases disappear, demonstrating the effectiveness of the treatment in protecting the substrate, forming an oxide coating (Al_2O_3).

The PEO coating consists mostly of aluminum (38.5°/44.8°/65°/78.5° and 82.5°), and gamma alumina (γ-Al_2O_3), formed by the transformation of amorphous alumina into a metastable phase (Eq. 2), due to microplasma discharges, which can reach 10,000 K of temperature in localized points, according to literature, such a phase is found when the coating created by plasma reaches at least 2 min of synthesis (Serdechnova, et al. 2017; Yang et al. 2019); therefore such peaks appear few times and with relatively small intensities in this study, and the magnesium present in the chemical composition of the substrate tends to reduce the amount of γ-Al_2O_3 present in the coating (Yang et al. 2019).
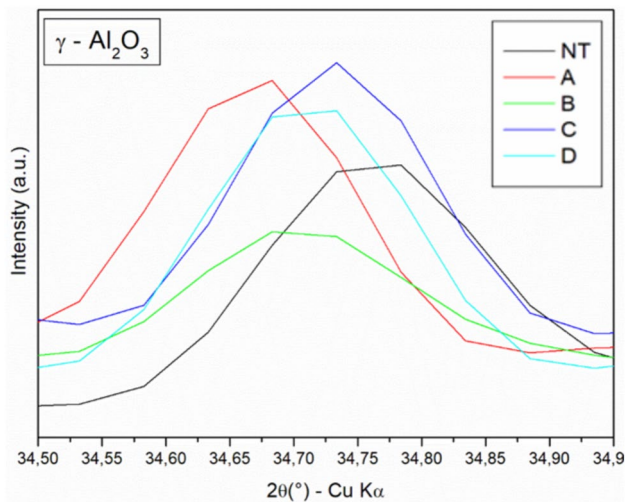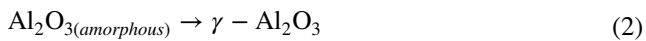
Fig. 6 Peak corresponding to the γ-Al_2O_3 phase

$$Al_2O_{3(amorphous)} \rightarrow \gamma - Al_2O_3 \tag{2}$$

Overlaying all the spectra and zooming in the region between 34.5° and 34.9° allows for a comparison of peak intensities related to the crystalline phase of γ-Al_2O_3 corresponding to the crystallographic plane [220], shown in Fig. 6.

The analysis revealed that the rise in electrolyte concentration led to the enhancement of the aluminum oxide coating up to its maximum point, except for treatment B (5 g/L). This phenomenon could be ascribed to the unevenness of the coating formation, potentially leaving some areas uncovered by the plasma. Moreover, the localized temperature experienced during the treatment might have facilitated the dissolution of the coating, alongside the existence of micro cracks that could expose the substrate, consequently reducing the presence of Al_2O_3 (Lucas et al. 2022; Sopchenski et al. 2020; Yang et al. 2019).

FT-IR Spectroscopy of the PEO Coating

Figure 7 shows the FT-IR spectra of the 2024 alloy, untreated, and after treatments with variation in electrolyte concentration.

In the spectrum, very weak bands are observed around 2320 cm^{-1}, relating to aromatic C=C and/or C=O functional groups absorbed from the environment. These functional groups are detected due to the concentration of Na^+ in the coating, originating from the electrolyte, which acts as a contaminant that enhances the adsorption capacity of CO_2 (Lucas et al. 2020, 2022; Fermine et al. 2023).

In the transmittance spectrum, hydroxyl functional groups are detected, indicating the presence of pseudoboehmite (AlOOH) at 1559 cm^{-1} and 1074 cm^{-1}. This is a result of the
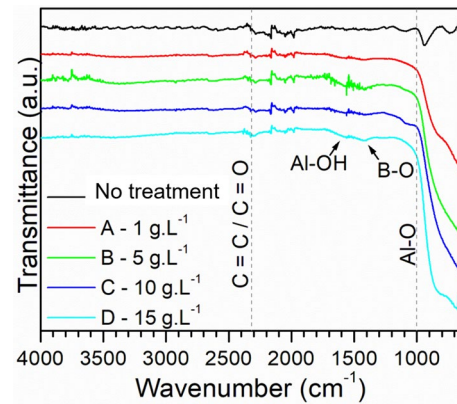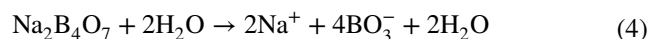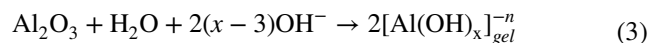

Fig. 7 FT-IR spectrum of 2024 treated by PEO

increased protective oxide coating on the substrates (Fermine, et al. 2023). Due to the ionic dissociation of tetraborate, functional groups related to borate ($B_4O_7^{-2}$) are observed in the coatings, thus demonstrating the difference from plasma treatment to conventional chemical and electrochemical processes, where the solution used does not contain additional elements from the coating (Yerokhin et al. 2004; Wierzbicka et al. 2022; Wierzbicka et al. 2021; Rameshbabu et al. 2022).

To explain the formation of pseudo-boehmite (AlOOH) and borate in the oxide coating, we can initially observe Eqs. 3 and 4, respectively. During plasma treatment, there is a considerable formation of oxygen around the anode, as well as phenomena related to the plasma, which favor the dissolution of the native oxide layer present on the substrate. From this dissolution, hydroxides are produced in the form of a gel, which, upon contact with the plasma surface, solidify (Lucas et al. 2022).

$$Al_2O_3 + H_2O + 2(x-3)OH^- \rightarrow 2[Al(OH)_x]_{gel}^{-n} \tag{3}$$

$$Na_2B_4O_7 + 2H_2O \rightarrow 2Na^+ + 4BO_3^- + 2H_2O \tag{4}$$

Functional groups found at 1000 cm^{-1} are related to the oxide layer (Al–O and Si–O–Si), found in the untreated substrate. Thus, the detected passive layer is also present in the plasma-treated substrates. It is noted that the addition of sodium tetraborate increases the alumina peaks, as the $B_4O_7^{-2}$ ions add oxygen to the ionized medium (Wierzbicka et al. 2021; Liu et al. 2021; Bai et al. 2019; Lucas et al. 2024).

Conclusion

With the treatment occurring potentiostatically (constant voltage), there is an abrupt drop in current in the system, a result of the formation of a dielectric oxide coating

(Al_2O_3) on the substrates. This, combined with plasma phenomena, increases the temperature of the electrolytic solution (Joule Effect).

Analyzing the data (voltage and current), the average power consumed in electrolytic and plasma treatments can be calculated. It is noted that an increase in conductivity decreases the average power consumed due to the "sparking" phenomenon occurring more rapidly, as well as the deposition rate.

The examination of the coatings' morphology revealed that the incorporation of sodium tetraborate ($Na_2B_4O_7$) led to the development of thin and dense coatings measuring 1.7 µm, a dimension that falls below what has been documented in previous literature. Moreover, characteristic features of PEO coatings, including microfissures generated by the swift solidification of the molten oxide upon contact with the electrolyte, as well as spherical protrusions and micro-pores stemming from electrical discharge pathways, were identified. An analysis using EDS demonstrates that the coating predominantly consists of aluminum (Al) and oxygen (O), culminating in the production of alumina (Al_2O_3), in addition to other constituents originating from the alloy and electrolyte, such as chromium (Cr), silicon (Si), and sodium (Na).

The efficacy of the PEO treatment is evident through the decrease in intermetallic phases (Al_2CuMg and Al_2Cu) identified via XRD in the untreated specimen, alongside the enhancement in the peak associated with ɣ-Al_2O_3, where it was noted that treatment C (10 g/L) displayed a superior peak in comparison to the other treatments. Nevertheless, peaks linked to aluminum are noticeable, attributed to the presence of fissures and/or voids within the oxide layer.

Analyzing the FT-IR spectra, functional groups of primitive alumina bonds are observed (Al_2O_3), as well as borate groups (BO^{-3}), highlighting the capability of electrolytic plasma to add elements present in the electrolyte to the coating. Stretching vibrations of OH groups were also observed at the beginning of the spectra. In this study, Na^+ ions acted as contaminants, favoring the adsorption of CO_2, which can promote the formation of bicarbonate ions and/or bidentate carbonate ions.

Data availability The authors confirm that the data supporting the findings of this study are available within the article [and/or] its supplementary materials.

Declarations

Conflict of interest The authors who participated in the development of this work declare that they have no conflicts of interest of any kind.

References

Ansari M et al (2018) Finite element analysis of AA1100 elasto-plastic behaviour using Johnson-Cook model. Mater Today Proc 5:5349–5353. https://doi.org/10.1016/j.matpr.2017.12.120

Bai S et al (2019) Influence of Sealing treatment on the corrosion resistance of PEO coated Al-Zn-Mg-Cu alloy in various environments. Coatings 867:1–13. https://doi.org/10.3390/coatings9120867

Dehnavi V et al (2013) Effect of duty cycle and applied current frequency on plasma electrolytic oxidation (PEO) coating growth behavior. Surf Coat Technol 226:100–107. https://doi.org/10.1016/j.surfcoat.2013.03.041

Duan H, Chuanwei Y, Fuhui W (2007) Effect of electrolyte additives on performance of plasma electrolytic oxidation films formed on magnesium alloy AZ91D. Electrochim Acta 52:3785–3793. https://doi.org/10.1016/j.electacta.2006.10.066

Fermine Y et al (2023) Combined atomic-scale/DFT-theoretical simulations and corrosion protection study of AA2024-T3 in 3.5% NaCl by phenolphthalein derivatives: surface characterization (FT-IR, FT-RAMAN, and SEM). J Electroanal Chem 943:117610. https://doi.org/10.1016/j.jelechem.2023.117610

Ghanaraja S et al (2018) Synthesis and study of microstructure and mechanical properties of cast Al1100 (Mg)–SiC composites. Mater Today Proc 5:2765–2772. https://doi.org/10.1016/j.matpr.2018.01.063

Khiabani A, Yarmand B, Mozafari M (2021) Enhanced corrosion resistance and in-vitro biodegradation of plasma electrolytic oxidation coatings prepared on AZ91 Mg alloy using ZnO nanoparticles-incorporated electrolyte. Surf Coat Technol 360:153–171. https://doi.org/10.1016/j.surfcoat.2019.01.002

Kikuchi T et al (2020) Fabrication of a plasma electrolytic oxidation/anodic aluminum oxide multi-layer film via one-step anodizing aluminum in ammonium carbonate. Thin Solid Films 697:137799. https://doi.org/10.1016/j.tsf.2020.137799

Liu J et al (2021) The corrosion inhibition effect of sodium silicate and Triton X-100 on 2024–T3 aluminum alloy in NaOH medium Experimental and theoretical research. Colloids Surf A 610:125723

Lucas R, Silva L, Santos D (2020) Morphological and chemical characterization of oxide films produced by plasma anodization of 5052 aluminum alloy in solution containing sodium silicate and sodium phosphate. Revista Brasileira De Aplicação No Vácuo. https://doi.org/10.17563/rbav.v39i1.1154

Lucas R et al (2022) Characterization of oxide coating grown by plasma electrolytic oxidation (PEO) at different times on aluminum alloy AA2024-T3. MRS Commun 12:266–271. https://doi.org/10.1557/s43579-022-00174-9

Lucas R et al (2024) Experimental design of the adhesion between a PEI/glass fiber composite and the AA1100 aluminum alloy with oxide coating produced via plasma electrolytic oxidation (PEO). Ceramics 7(2):596–606. https://doi.org/10.3390/ceramics7020039

Mengesha G et al (2020) Effects of processing parameters on the corrosion performance of plasma electrolytic oxidation grown oxide on commercially pure aluminum. Metals 10:394. https://doi.org/10.3390/met10030394

Mohedano M et al (2021) Effects of pre-anodizing and phosphates on energy consumption and corrosion performance of PEO coatings

on AA6082. Surf Coat Technol 409:126892. https://doi.org/10.1016/j.surfcoat.2021.126892

Rameshbabu N et al (2022) Surface characteristics of AC PEO coatings fabricated on commercial Al alloys. Surf Coat Technol 449:128975. https://doi.org/10.1016/j.surfcoat.2022.128975

Reis J et al (2021) Feasibility study of the oxy fuel gas welding (OFW) process in AA2024-T3 and GF/PEI composite hybrid joint. Weld World 65:1145–1160. https://doi.org/10.1007/s40194-021-01091-6

Serdechnova M et al (2017) PEO coatings with active protection based on in-situ formed LDH-nanocontainers. J Electrochem Soc 164:36–45. https://doi.org/10.1149/2.0301702jes

Shore D et al (2021) Adhesive bond strength of PEO coated AA6060-T6. Surf Coat Technol 428:127898. https://doi.org/10.1016/j.surfcoat.2021.127898

Sopchenski L et al (2020) Improvement of wear and corrosion protection of PEO on AA2024 via sol-gel sealing. Surf Coat Technol 417:127195. https://doi.org/10.1016/j.surfcoat.2021.127195

Wierzbicka E et al (2021) Flash-PEO as an alternative to chromate conversion coatings for corrosion protection of Mg alloy. Corros Sci 180:109189. https://doi.org/10.1016/j.corsci.2020.109189

Wierzbicka E et al (2022) Chromate-free corrosion protection strategies for magnesium alloys—a review: part II—PEO and anodizing. Materials 15:8515. https://doi.org/10.3390/ma15238515

Xue W et al (2014) Discharge behaviors during plasma electrolytic oxidation on aluminum alloy. Mater Chem Phys 148:284–292. https://doi.org/10.1016/j.matchemphys.2014.07.045

Yang Z et al (2019) An interesting anodic oxidation behavior of plasma electrolytic oxidation coatings fabricated on aluminum in alkaline phosphate electrolyte. Surf Interfaces 16:199–205. https://doi.org/10.1016/j.surfin.2018.10.004

Yerokhin A et al (1999) Plasma eletrolysis for surface engineering. Surf Coat Technol 122:73–93. https://doi.org/10.1016/S0257-8972(99)00441-7

Yerokhin A et al (2004) Spatial characteristics of discharge phenomena in plasma electrolytic oxidation of aluminium alloy. Surf Coat Technol 177:779–783. https://doi.org/10.1016/j.surfcoat.2003.06.020

Zinigrad M, Kossenko A (2015) A universal electrolyte for the plasma electrolytic oxidation of aluminum and magnesium alloys. Mater Des 88:302–309. https://doi.org/10.1016/j.matdes.2015.08.071